Simulation Modelling Practice and Theory 23 (2012) 36–59

Contents lists available at SciVerse ScienceDirect

Simulation Modelling Practice and Theory

journal homepage: www.elsevier.com/locate/simpat

Detailed modelling, implementation and simulation of an "all-in-one" stability test system including power system protective devices

Rujiroj Leelaruji, Luigi Vanfretti *

KTH Royal Institute of Technology, School of Electrical Engineering, Electric Power Systems, Teknikringen 33, Stockholm, Sweden

ARTICLE INFO

Article history:
Received 28 June 2011
Received in revised form 6 December 2011
Accepted 9 January 2012
Available online 1 February 2012

Keywords:
Power system simulation
Power system modelling
Power system stability
Protection systems
PowerFactory

ABSTRACT

This paper presents modelling and simulation results for multiple instability scenarios of the "all-in-one" test system. The test system is an alteration of the Bonneville Power Administration test system constructed to capture transient (angle), frequency and voltage instability phenomena, resulting in system collapse, within one system. The paper describes general overview of the test system and its associated individual devices modelling. These modelling are both customized and adapted from the built-in model developed by PowerFactory simulation software. The paper also provides a description of different instabilities that can be reproduced by this self-contained system. One of the case study is demonstrated in detail with the necessary initialization settings for reproducing instability scenario.

1. Introduction

The different synchronous systems in the European Network of Transmission System Operators for Electricity (ENTSO-E) have experienced a chain of severe power system failures evidencing that these power systems are currently being operated under more stringent conditions. This fact motivates a search for methods capable of preventing severe failures or at least mechanisms to decrease the risk of blackouts. Large blackouts are the result of a complex sequence of component failures [1], equipment misoperations [2], unintended operator actions [3] and human error [4]. These complex sequence of events are commonly referred to as cascading failure or rolling blackouts. Cascading failures are rare because the most likely contingencies are considered beforehand in power system planning design and operational routines. It can be argued that with a high degree of the "controllability" in the power system, cascading failures can be mitigated or even completely avoided. This kind of controllability is raising with the increased number of installations of FACTS devices and VSC-HVDC systems. On the other hand, protective devices commonly act as the last resource to guarantee personnel and equipment safety, however under certain circumstances they might misoperate, initiating a rolling blackout.

The authors hypothesize in [5] that if the operation of protective devices is coupled to the potential relief capacity of power system controllable devices, then cascading failures can be avoided. To this aim, controls mechanisms coupling protection systems and power system controls can be developed to fulfil this aim. The first steps to develop such algorithms are to elaborate a test system which is able to reproduce all possible instability scenarios, and that at the same time, contains calibrated protective devices that act according to conventional protective relaying principles. Such test system can be used as a basis to develop the control mechanisms that consider both the conventional operation of protective relays and the

* Corresponding author.
E-mail addresses: luigi.vanfretti@ee.kth.se, luigiv@kth.se, lvanfretti@ieee.org (L. Vanfretti).

1569-190X/$ - see front matter © 2012 Elsevier B.V. All rights reserved.
doi:10.1016/j.simpat.2012.01.002

operation and physical constraints of power system controllable devices. To fulfil these requirements, the test system must be developed with care, paying attention to important modelling details of each power system component, it's controls, and associated protective devices.

The objective of this paper is to perform detailed modelling and implementation of a test system that is capable of generating different instability scenarios. The test system is an alteration of the Bonneville Power Administration (BPA) test system which was originally implemented in a special toolbox developed in the MATLAB/Simulink®platform [6], in this article a completely new realization in PowerFactory has been implemented. Each individual device model is described in detail and mapped to different implementation approaches available within a commercial and proprietary simulation software.[1] A detailed example of a instability scenario is given with its initialization settings to show the need of accurate implementation of the different device models in the system. The detailed modelling of each device is necessary for developing algorithms capable of coordinating the operation of protective devices with power system controls in order to enhance the stability of power systems.

In view of the description above, the contributions of this paper can be summarized as follows:

- To perform detailed modelling and implementation of a test system capable of generating different instability scenarios, and including protective relays, within a commercial and proprietary software, i.e. the "all-in-one" system.
- To explain how built-in models which are implemented within the software's library can be modified to satisfy the user's modelling requirements.
- To illustrate different model implementation approaches that can be used within a commercial and proprietary software tool to implement specific customized user defined models which are necessary for the representation of important system dynamic behaviour.
- To demonstrate, through simulations, how the adapted and customized models are capable of accurately capturing power system dynamic behaviour.
- To exhibit the different relay coordination considerations that must be taken into account when specifying the protective device settings for the test system in this paper.
- To implement protective relay models within the test system that are capable of operating according to conventional power system protection design requirements.
- To show, through simulations, that the relay models implemented in the test system operate according to the design specifications considered within this study.

The remainder of this paper is organized as follows. Section 2 describes the power system models and their implementation in the DIgSILENT PowerFactory software. Section 3 describes instability scenarios that can be simulated by the "all-in-one" system. In Section 4, considerations for the design of protective relays and steps for their modelling and implementation in the "all-in-one" system are discussed. In Section 5 conclusions are duly drawn.

2. System modelling

The commercial and proprietary DIgSILENT PowerFactory simulation software offers a Graphical User Interface (GUI) to implement power system models for stability analysis purposes. The software is complemented with a library that contains built-in IEEE models, and it also allows users to create their own models if needed. The models can be implemented by either building block diagrams or programming in the DIgSILENT Simulation Language (DSL) block definitions; allowing for the representation of transfer functions, or differential equations for the more complex transient models. This section presents a test power system and the detailed models of each individual device implemented in PowerFactory by using block diagrams and DSL programming.

2.1. Test system

A one-line diagram of the "all-in-one" test system is shown in Fig. 1. The system consists of a local area connected to a strong grid (Thevenin Equivalent) by two 380 kV transmission lines. A motor load (rated 750 MVA, 15 kV) is connected at Bus 4 and supplied via a 380/15 ratio transformer. A load with constant power characteristics and load tap changer (LTC) dynamics at the distribution side are explicitly modelled at Bus 5. A local generator (rated 450 MVA, 20 kV) is connected at Bus 2 to supply the loads through a 20/380 ratio transformer.

From the power system viewpoint, excitation systems should be capable of responding rapidly to a disturbance so that proper voltage support is provided through excitation control. Thus, excitation systems should be designed to have a fast acting response to enhance transient stability. This fast response requirement has been taken into consideration by manufactures which have developed excitation control systems, such as the GE EX2100 [8], Westinghouse's static excitation system [9], and others, that can be modelled through the IEEE Type ST excitation models recommended by the IEEE Standard

[1] For definitions of software categories such as "commercial" and "proprietary" please refer to [7].

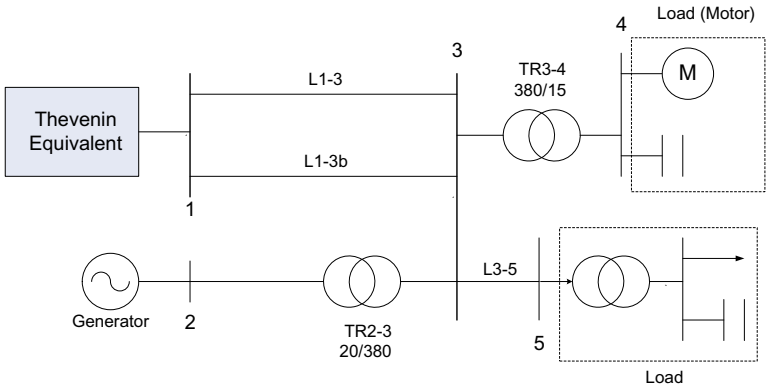

Fig. 1. "All-in-one" test system.

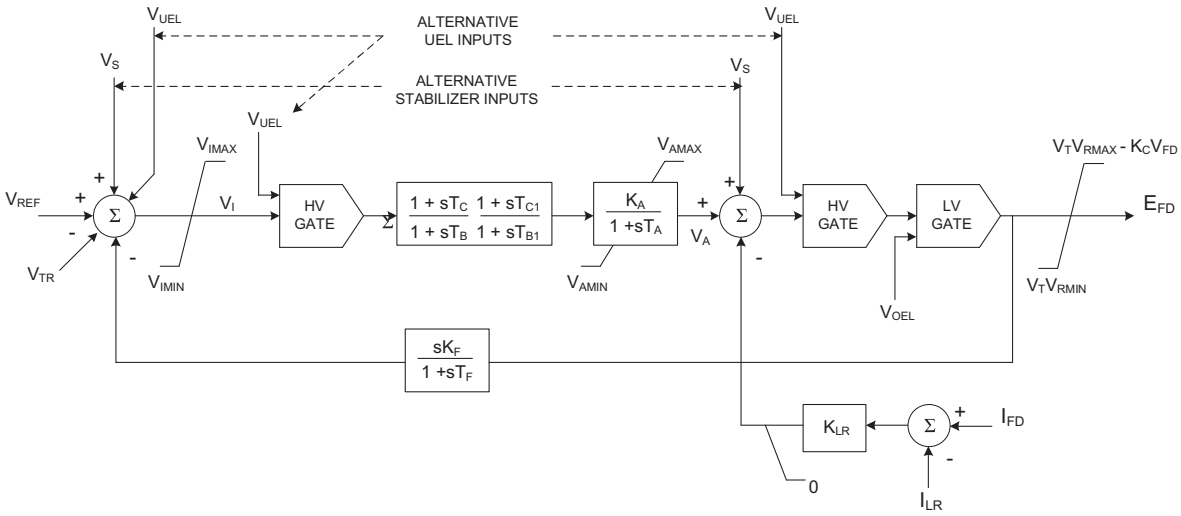

Fig. 2. ST1A excitation system block diagram showing major functional blocks (adapted from Ref. [10]).

421.5 [10]. In this study, the ST1A model (shown in Fig. 2) is implemented by setting model parameters to appropriate values, then simplifications are made.

2.2. Adapting built-in models

This section describes an approach to adapt built-in models already implemented in the PowerFactory software to meet the modelling requirements that allow the "all-in-one" test system to reproduce different instability scenarios.

- The *simplified ST1A excitation system* is implemented by setting time constants T_B, T_{B1}, T_C and T_{C1} in the forward path of the original ST1A excitation system to zero. The internal excitation control system stabilization is represented in the feedback path with the gain K_F (internal limits on V_I and the internal feedback stabilization time constant (T_F) are neglected in this paper). This is a suitable practice in many cases as stated in Ref. [10]. Moreover, the current limit (I_{LR}) and gain K_{LR} of the field current limiter are set to zero. An underexcitation limiter (V_{UEL}) input voltage is also ignored, nevertheless an overexcitation limiter (V_{OEL}) is added at the first summation junction instead of the low voltage gate.
  Fig. 3 depicts the excitation system obtained from the simplifications above, and used in this study. The input signal of the excitation system is the output of the voltage transducer, V_{TR}. This voltage is compared with the voltage regulator reference, V_{REF}. Thus, the difference between these two voltages is the error signal which drives the excitation system. An additional signal from overexcitation limiter (OEL) output, V_{OEL}, becomes non-zero only under abnormal operating conditions. To realize this model within the built-in models already implemented in the PowerFactory software, model parameters can be set as shown in Fig. 4.

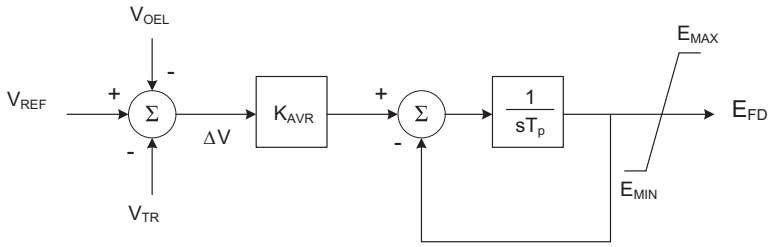

Fig. 3. Simplified excitation system model obtained by simplifying the IEEE ST1A excitation model.

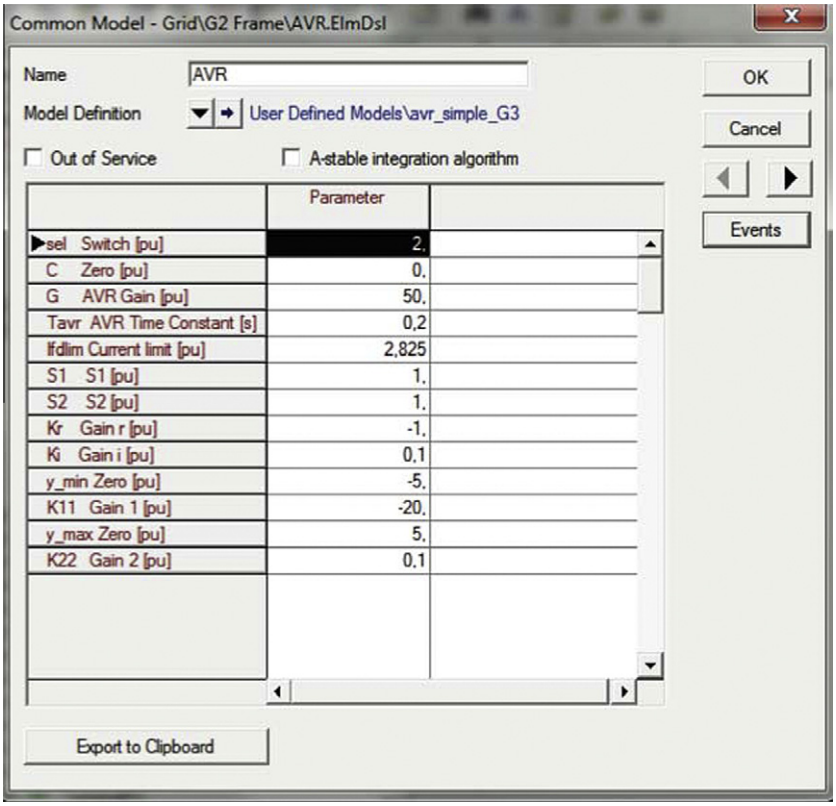

Fig. 4. Parameter settings for representing the AVR model of Fig. 3 in the PowerFactory software.

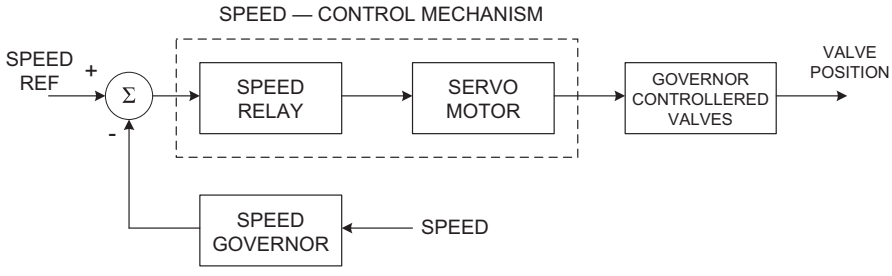

Fig. 5. Functional block diagram of a typical speed-governing system.

- A typical *speed-governing system* consists of a speed governor, a speed relay, hydraulic servomotors, and controlled valves, which are represented in the functional block diagram in Fig. 5.
  The speed-governor regulates the speed of a generator by comparing its output with a predefined speed reference, the resulting error signal is sent to and amplified by a speed relay (a shaft speed is transformed into a valve position). The servomotor is necessary to move steam values (especially, in case of large turbines) and can be considered as an amplification. A standard model that can be used to represent a mechanical-hydraulic system as shown in Fig. 6, can be found in an IEEE Working Grouping Report [11]. This model is altered by many manufacturers, such as GE and Westinghouse, by applying different governor time constant (T_1), governor derivative time constant (T_2), and servo time constant (T_3). In this study, the Westinghouse EH Without Steam Feedback [11] is considered. To implement this model in PowerFactory; T_1, T_2, and T_3 are set to 0, 0, and 0.1, respectively. The valve speed (open or close) is determined by maximum and minimum rate of change of the valve position (Z'_{MAX} and Z'_{MIN}, respectively) where the gate position is limited by maximum and minimum gate position (P_{MAX} and P_{MIN}, respectively). To realize this model within the built-in models already implemented in the PowerFactory software, model parameters can be set as shown in Fig. 7.
- A *steam turbine* converts stored energy from high pressure and temperature steam into rotating energy, which in turn is converted into electrical energy by a generator. The general model used for representing steam turbines is provided in [11]. This model is applicable for common steam turbine system configurations which can be characterized by an appropriate choice of model parameters. A steam system, tandem compound single reheat turbine, was selected for this study (shown in Fig. 8). This turbine is represented by a simplified linear model [11], which is shown in Fig. 9.

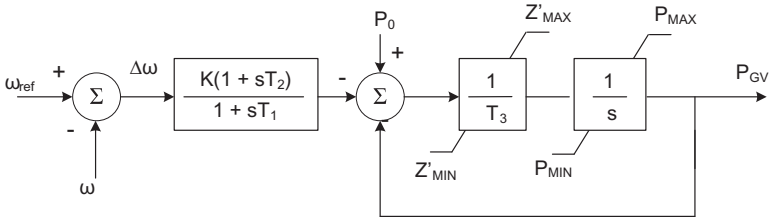

Fig. 6. Model for the speed-governing system of the steam turbine.

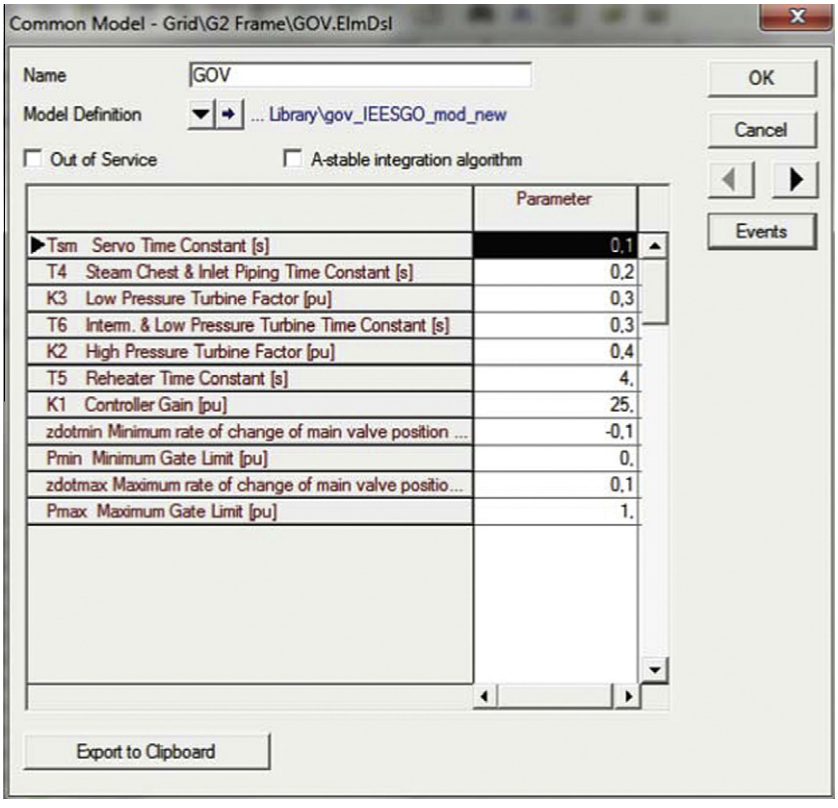

Fig. 7. Parameter settings for representing the speed-governing model of Fig. 6 in the PowerFactory software.

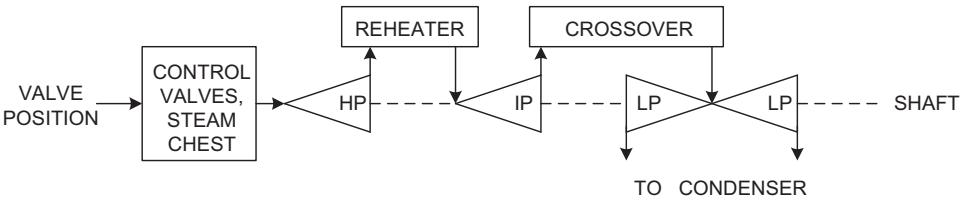

Fig. 8. Steam turbine configuration.

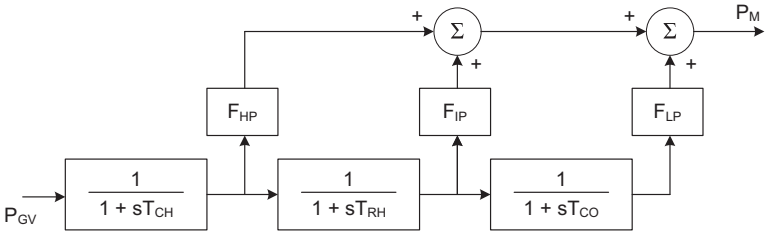

Fig. 9. Approximate linear model representing the turbine in Fig. 8.

From Fig. 8, steam enters the high pressure (HP) stage through the control valves and the inlet piping. The housing for the control valves is called "steam chest". Then, the HP exhaust steam is passed through a reheater. Physically, this steam returns to the boiler to be reheated for improving efficiency before flowing into the intermediate pressure (IP) stage and the inlet piping. Subsequently, the crossover piping provides a path for the steam from the IP section to the low pressure (LP) inlet. In this paper, Fig. 10 shows the models implementation in PowerFactory. It depicts the steam turbine with speed governor where the left-block and right-block represent speed governing system and steam turbine, respectively. This model was implemented by modifying PowerFactory's "gov_ IEESGO_ mod_ new: IEEE Standard Governor" model, where the speed governing system did not reflect the recommendations in [11]. Hence the speed-governing system was modified by replacing the lead-lag and the first-order delay filter with gain blocks by a constant block. Moreover, the limiter block in the original built-in model is replaced by a constant with limiter and the limited non-windup integrator blocks. Finally, the output signal from integrator block is added at the second summation junction. Fig. 11 shows a comparison between the speed-governing system before and after the necessary modifications performed for this study.

2.3. Custom models

This section describes the modelling and implementation of user defined customized devices that are necessary for simulating instability scenarios using the "all-in-one" system. For example, an overexcitation limiter, a load tap changer, and a load restoration model are required to illustrate voltage instability phenomena. Since they were not available in PowerFactory, they were implemented by using DSL programming and block diagrams.

- An *overexcitation limiter (OEL)* model is necessary to capture slow phenomena, such as voltage instability, which may force machines to operate at high excitation levels over long periods. According to the IEEE recommended practice 421.5 [10], OELs are required in excitation systems to capture slow changing dynamics associated with long-term phenomena. The OEL's purpose is to protect generators from overheating due to persistent and larger field currents that are beyond design limits. This can be caused either by the failure of a component inside the voltage regulator, or an abnormal system condition. In other words, it allows machines to operate for a defined time period in overload conditions, and then reduces the excitation to a safe level. A standard model that can be used to implement most OELs can be found in [12]. In this study, an OEL is modelled and implemented following the block diagram shown in Fig. 12.
  The OEL detects high field currents (I_{FD}) and outputs a voltage signal (V_{OEL}), which is sent to the excitation system summing junction. This signal is equal to zero in normal operation conditions. In other words, V_{OEL} is zero if I_{FD} is less than $I_{FD\ lim}$. As a result the error signal (ΔV) is altered so that the field current is decreased below overexcitation limits (forces I_{FD} to I_{FDlim}). As shown in Fig. 12, Block 1 is a two-slope gain obeying the following expressions.

$$x_2 = S_1 x_1 \quad \text{if } x_1 \geqslant 0, \tag{1}$$

$$= S_2 x_1 \quad \text{otherwise}. \tag{2}$$

With S_1 and S_1 greater than zero, Block 2, the non-windup limited integrator block reacts as the following expressions.

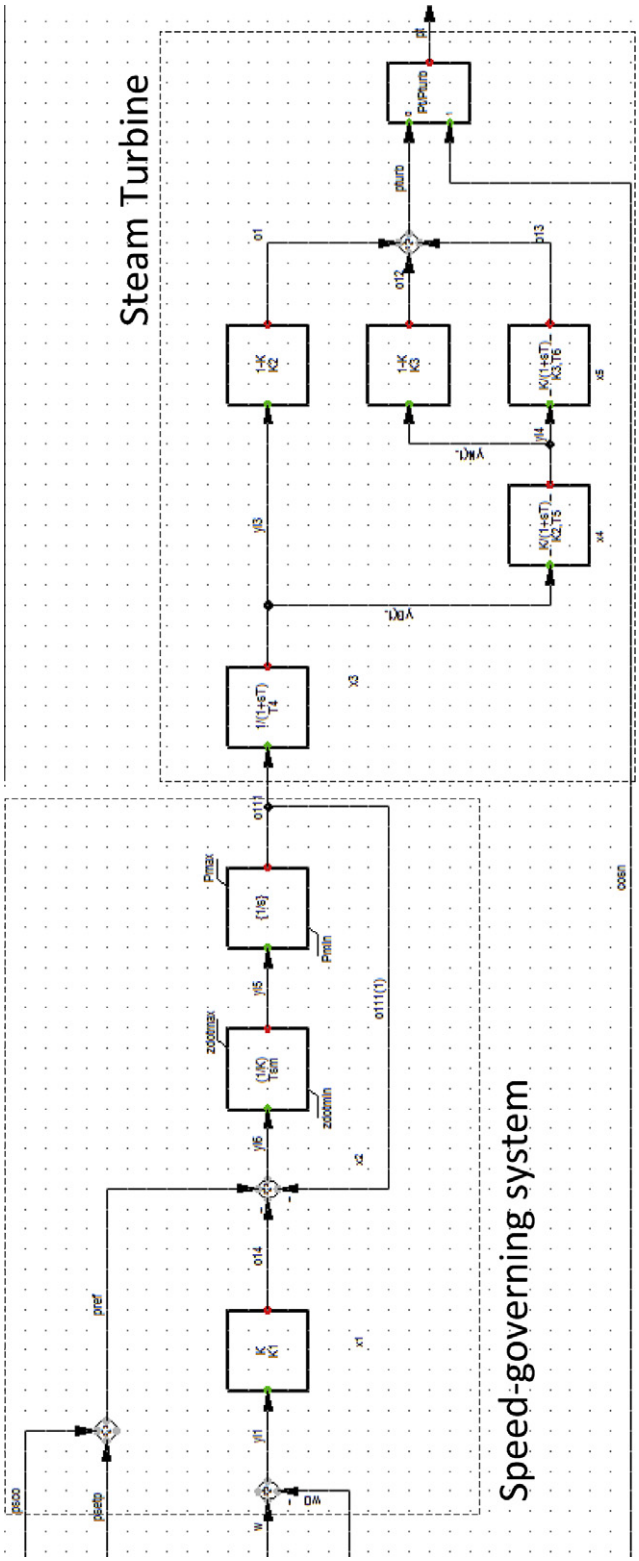

Fig. 10. Steam turbine with speed governor modelled in PowerFactory.

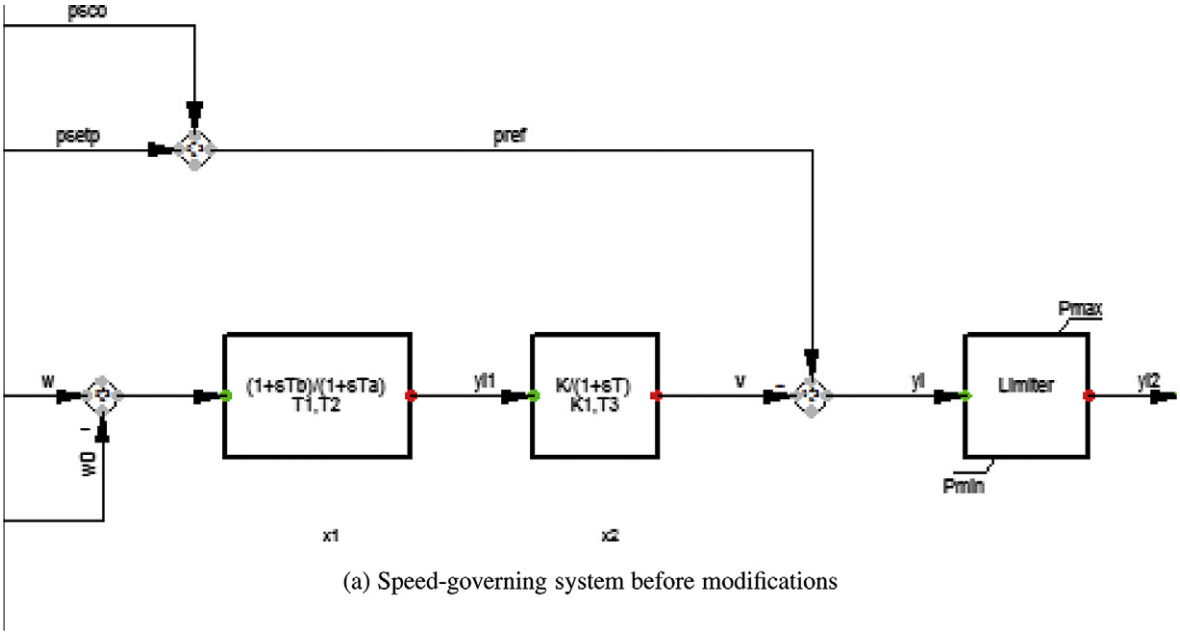

(a) Speed-governing system before modifications

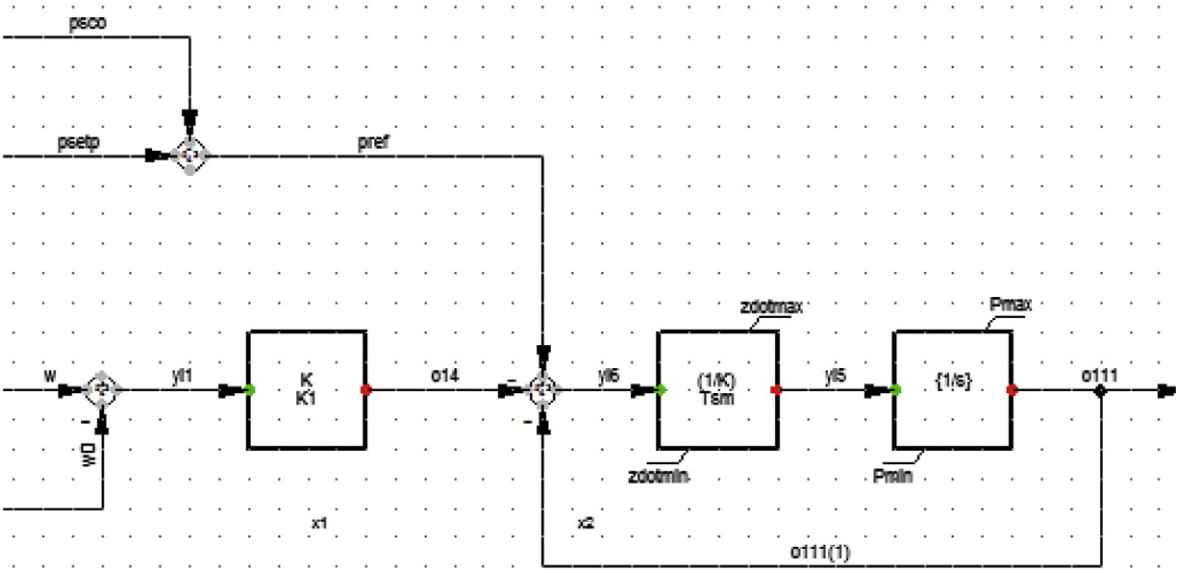

(b) Speed-governing system after modifications

Fig. 11. Comparison of speed-governing system before and after modifications.

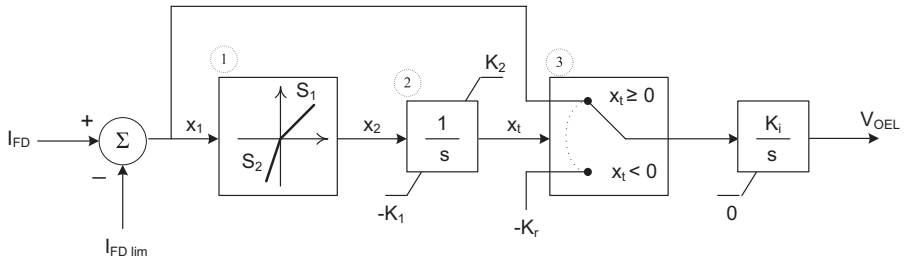

Fig. 12. Overexcitation limiter (adapted from Ref. [13]).

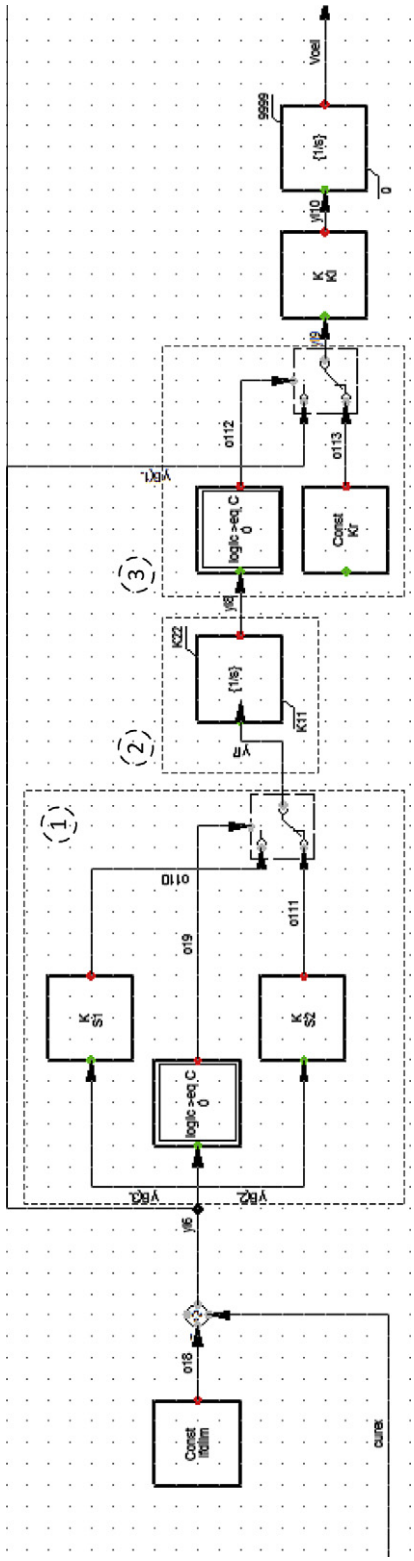

Fig. 13. Overexcitation limiter implementation in PowerFactory software.

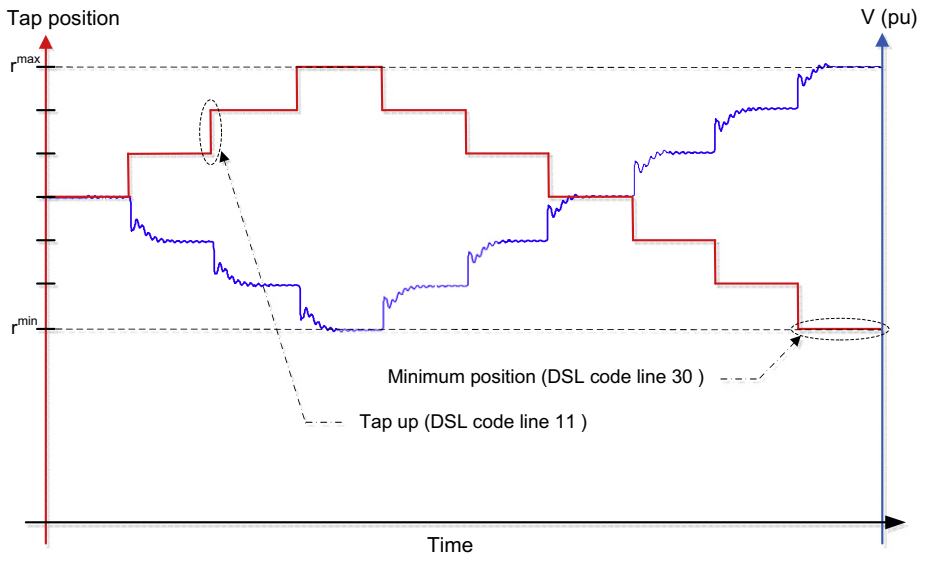

Fig. 14. Example of LTC's tap position movement.

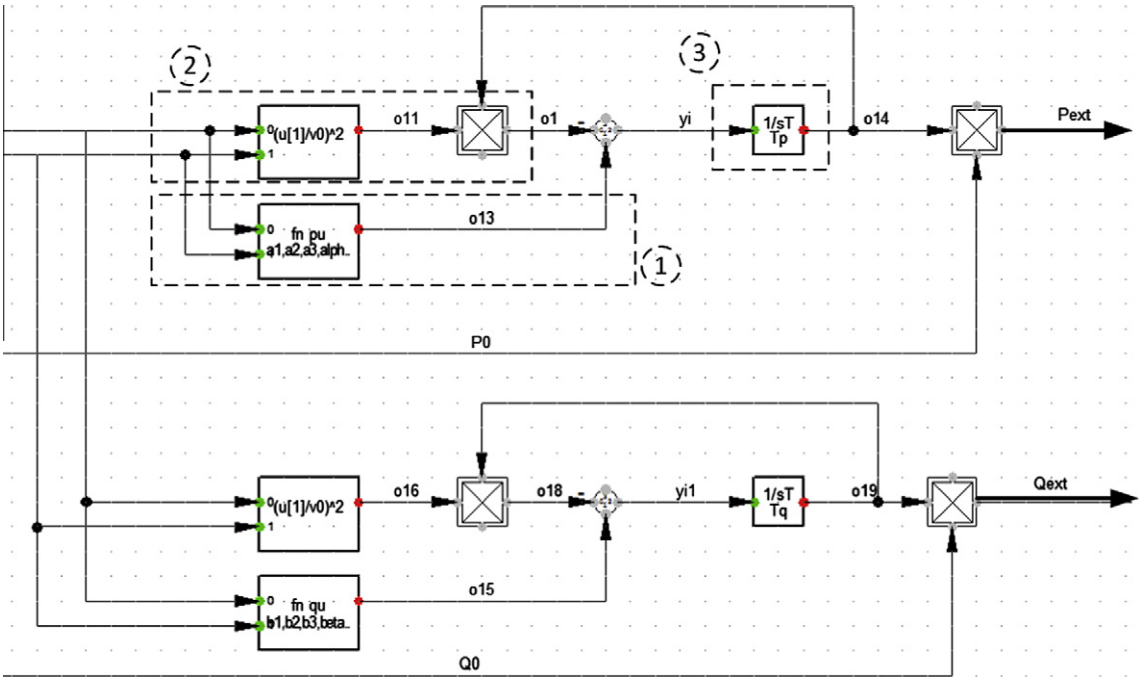

Fig. 15. Load restoration model implemented in PowerFactory software.

$$\dot{x}_t = 0 \quad \text{if } (x_t = K_2 \text{ and } \dot{x}_2 \geqslant 0) \text{ or } (x_t = -K_1 \text{ and } \dot{x}_2 < 0), \tag{3}$$

$$= x_2 \quad \text{otherwise.} \tag{4}$$

Assume that I_{FD} becomes larger than $I_{FD\ lim}$, this means that x_t is also greater than zero. Thus, Block 3 switches as indicated in Fig. 12 and the signal is sent to the wind-down limited integrator to produce V_{OEL}. Large values of S_2 and K_r cause V_{OEL} to return to zero when I_{FD} is less than $I_{FD\ lim}$. The OEL model implemented in PowerFactory software is shown in Fig. 13 where block numbers 1, 2, and 3 (outlined by a dashed line and numbered in circles) represent the two-slope gain, the non-windup limited integrator, and the switching blocks which behave similarly as an OEL presentation shown in Fig. 12, respectively.

- *Load tap changer (LTC)* transformers automatically operate to maintain voltages at loads within desired limits, especially when the system is under disturbances. In other words, LTCs act to restore voltages by adjusting transformer taps. As a result the voltage level will progressively increase to its pre-disturbance level. Dynamic characteristics of an LTC's logic can be modelled in different ways, as described in CIGRE Task Force 38-02-10 [14]. In this paper, a discrete LTC model is chosen, its function is to raise or lower the transformer ratio by one tap step. The tap changing logic at a given time instant is modelled by Van Cutsem and Vournas [13]:

$$r_{k+1} = \begin{cases} r_k + \Delta r & \text{if } V > V^0 + d \text{ and } r_k < r^{max} \\ r_k - \Delta r & \text{if } V < V^0 - d \text{ and } r_k > r^{min} \\ r_k & \text{otherwise} \end{cases} \tag{5}$$

where Δr is the size of each tap step, k is the tap position, and r^{max}, r^{min} are the upper and lower tap limits, respectively. The LTC is activated when the voltage error increases beyond one half of the LTC deadband limits (d). To this aim, a comparison between the controlled voltage (V) and the reference voltage (V^0) is performed by the LTC's logic:

$$k = 0 \text{ if } \left|V(t_0^+) - V^0\right| > d \text{ and } \left|V(t_0^-) - V^0\right| \leqslant d \tag{6}$$

Moreover, the tap movement can be categorized into two modes which are: *sequential*, and *non-sequential* [15]. In this study, the sequential mode is adopted. Here the first tap position changes after an initial time delay and continues to change at constant time intervals. If the transformer ratio limits are not met, the LTC will bring the error back inside into the deadband. The LTC can be

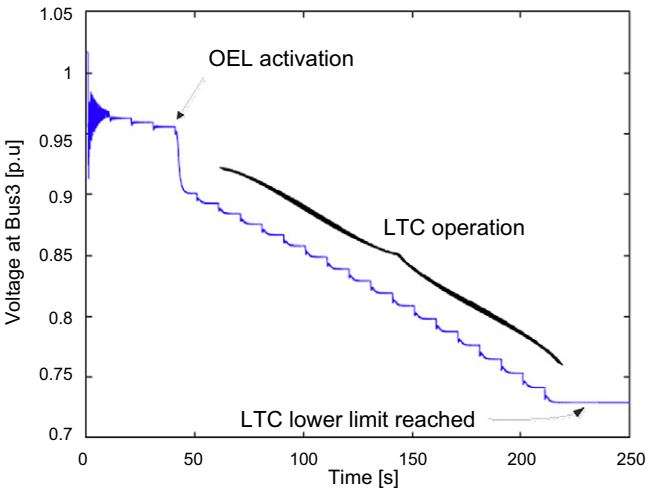

(a) Load = 1500 MW and 150 MVAR

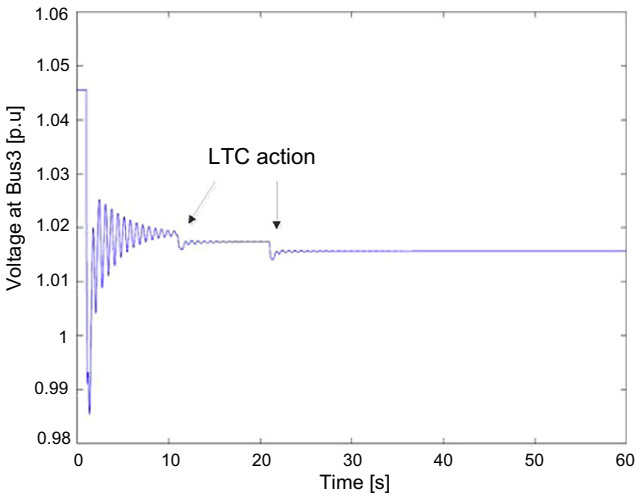

(b) Load = 1200 MW and 0 MVAR

Fig. 16. Voltage at Bus 3.

modelled in PowerFactor software by using DIgSILENT Simulation Language (DSL) code that offers some flexibility for implementing user-specific models need for stability analysis purposes [16]. The DSL code for LTC modelling is shown in Appendix A. This code can be mapped to the example in Fig. 14 provided to illustrate how the LTC's tap position can be controlled.
From the code shown in Appendix A, line 1–6 represent the initial conditions requirement for voltage level and transformer's tap position. Line 8–12 represent the movement of tap position. The example shown in Fig. 14 that code in line 11 implements the first condition described in (5). Next, the code in line 14–22 represent the first tap movement. The code in line 24–25 describes how the subsequent taps are performed at a constant time where line 27–28 represent the DSL programming requirement in order to move tap up or down. Code in line 30 is implemented to check the tap position reaches the minimum limit as shown in Fig. 14. The comparison between the controlled voltage and reference voltage described in (5) is performed by DSL code in line 35–38. Meanwhile, code in line 39–44 is for setting parameter values such as minimum tap position or LTC's half deadband.

- A *load restoration model* in this paper is a generic type self-restoring load in which load dependencies on terminal voltages exhibit power restoration characteristics. Generic load models can be categorized into two types which are *multiplicative* and *additive*, in these models the load state variable is multiplied and added to a transient characteristic. In this study, a multiplicative generic load model is selected, the load power is given by Van Cutsem and Vournas [13]:

$$P = z_P P_0 \left(\frac{V}{V_0}\right)^{\alpha_t}, \tag{7}$$

$$Q = z_Q Q_0 \left(\frac{V}{V_0}\right)^{\beta_t}, \tag{8}$$

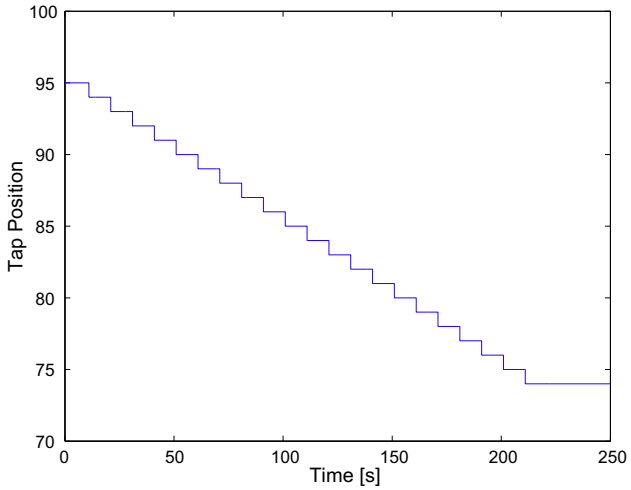

(a) Load= 1500 MW and 150 MVAR

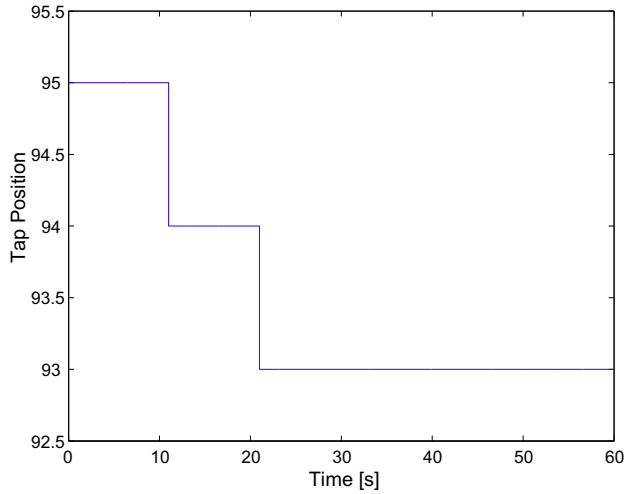

(b) Load= 1200 MW and 0 MVAR

Fig. 17. LTC Transformer tap position.

where z_P and z_Q are dimensionless state variables associated with load dynamics and $z_P = z_Q = 1$ in steady state. Moreover, the dynamics of the multiplicative model are described by:

$$T_p \dot{z_P} = \left(\frac{V}{V_0}\right)^{\alpha_s} - z_P \left(\frac{V}{V_0}\right)^{\alpha_t}, \tag{9}$$

$$T_Q \dot{z_Q} = \left(\frac{V}{V_0}\right)^{\beta_s} - z_P \left(\frac{V}{V_0}\right)^{\beta_t}, \tag{10}$$

where T_P and T_Q are restoration time constants for active and reactive load, respectively. The steady state active and reactive load-voltage dependencies are characterized by α_s and β_s, respective. Meanwhile, the transient active and reactive load-voltage dependencies are characterized by α_t and β_t, respectively. The load restoration model implemented in PowerFactory for this study is shown in Fig. 15. In this figure (for active load), Blocks 1 and 2 represent the first and second term on the right-handed side of (9), respectively. The voltage V_0 is set to the voltage bus at initial condition (see Appendix) and the voltage V is the measured bus voltage. Other parameters such as α_s, α_t, and T_P (in Block 3) are defined by DSL programming as described in LTC section. The equation for reactive power load follows the same form.

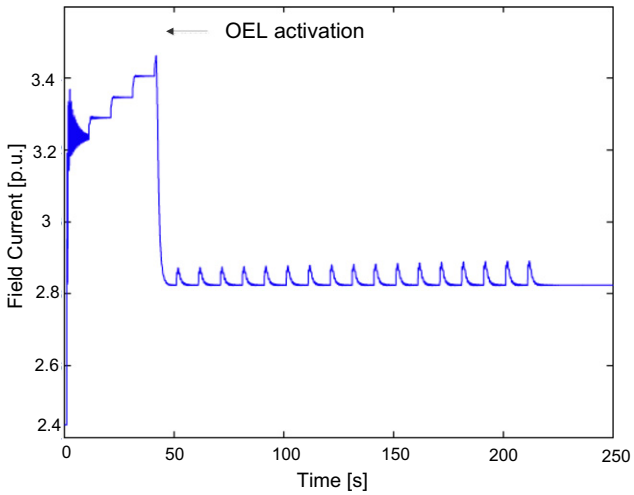

(a) Load = 1500 MW and 150 MVAR

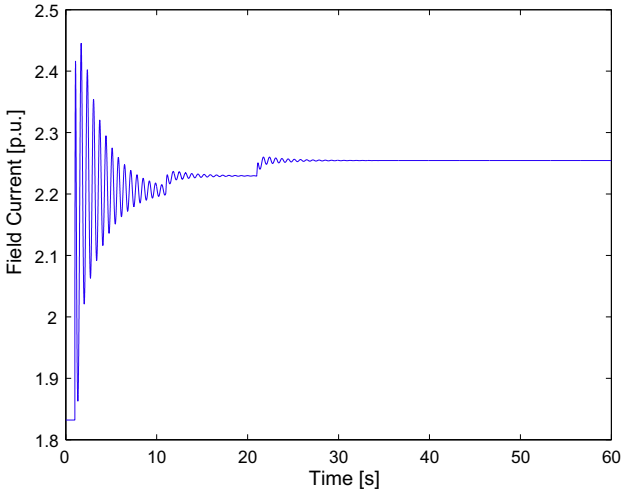

(b) Load = 1200 MW and 0 MVAR

Fig. 18. Generator field current.

3. Simulation of instability scenarios

Voltage stability is defined by the IEEE/CIGRÉ Joint Task Force on Stability Terms and Definitions [17] as *"the ability of a power system to maintain steady voltages at all buses in the system after being subjected to a disturbance from a given initial operating condition. It depends on the ability to maintain/restore equilibrium between load demand and load supply from the power system. Instability that may result occurs in the form of a progressive fall or rise of voltages of some buses"*. In the same document, voltage stability is categorized in two groups depending on the time frame in which the phenomena takes place, these are: (i) short-term voltage stability and (ii) long-term voltage stability. In this paper, a detailed example is described to demonstrate how a long-term voltage instability takes place. In order to simulate this phenomena, some initialization settings must be fulfilled as shown in Appendix B, and in this example the motor load is disconnected. Section 4.2 will show a different scenario where the motor load is connected.

In this case, one of the transmission lines between Bus 1 and 3 is tripped at $t = 1$ s. The overexcitation limiter (OEL) at the generator is triggered, thus generator's voltage is no longer controlled. Consequently, the LTC unsuccessfully attemps to restore the load bus voltage, until reaches its lower limit. Fig. 16a shows the load bus voltage decreases stepwise accordingly. This is a long-term voltage instability scenario compared to a case when load is decreased from 1500 MW and 150 MVAR to 1200 MW and 0 MVAR, shown in Fig. 16b. The load tap changer (LTC) is capable of restoring the voltage at the load bus within its deadband (see Fig. 16b). This forces the power system to operate at a new

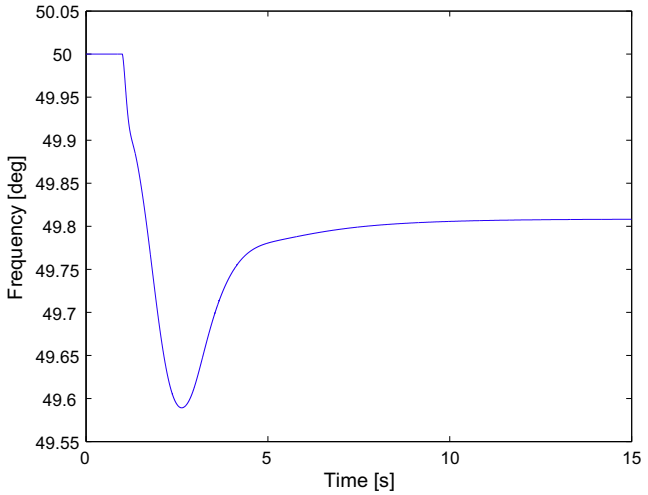

(a) Load = 400 MW

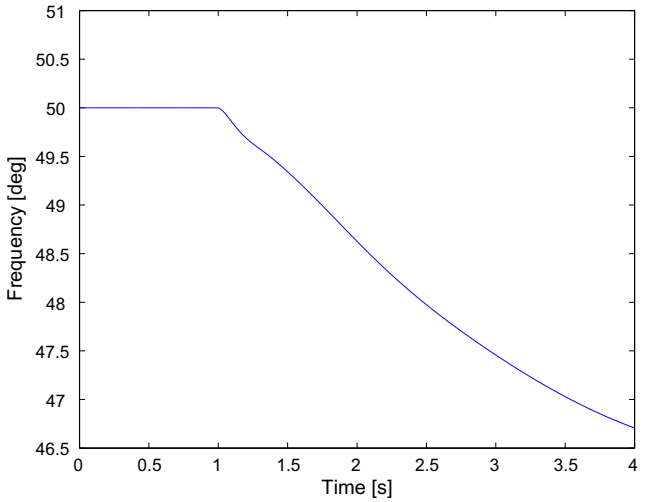

(b) Load = 500 MW

Fig. 19. Generator frequency.

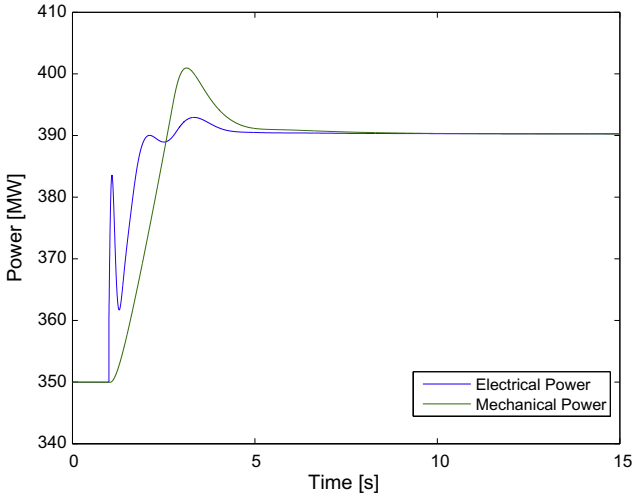

(a) Load= 400 MW

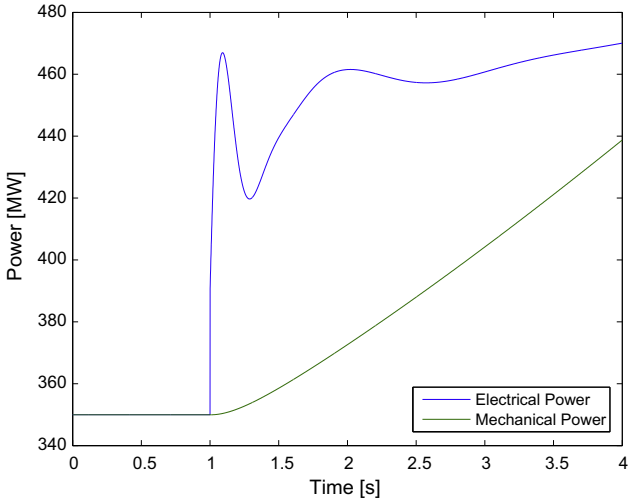

(b) Load= 500 MW

Fig. 20. Generator electrical and mechanical power.

equilibrium point. In addition, Figs. 17 and 18 show the transformer tap position and field current of the generator at different load levels.

As mentioned in Section 1, the "all-in-one" system can be used for simulating different instability scenarios by setting different parameters and initial (load flow) conditions. All possible instability scenarios can be generated with this test system, they are throughly documented in [18]. One of the scenarios is a frequency instability scenario which can be simulated by setting the load restoration to 500 MW and the generator capacity to 450 MW, and tripping two transmission lines between Bus 1 and 3. This load cannot be supplied by the generator when the system is isolated from the Thevenin equivalent. Hence, frequency decay cannot be stopped, resulting in frequency instability. Fig. 19a depicts the case of frequency restoration by the governor, whereas Fig. 19b shows how the governor attempts to overhaul the frequency but it fails. In addition, Fig. 20a and b shows the power mismatch between electrical power and turbine mechanical power in the case when the load equals to 400 and 500 MW, respectively.

4. Relay settings

The problem of coordinating protective relays in electric power systems is to select their suitable settings such that their fundamental protective function is achievable under some requirements, for example, sensitivity, selectivity, and speed. This

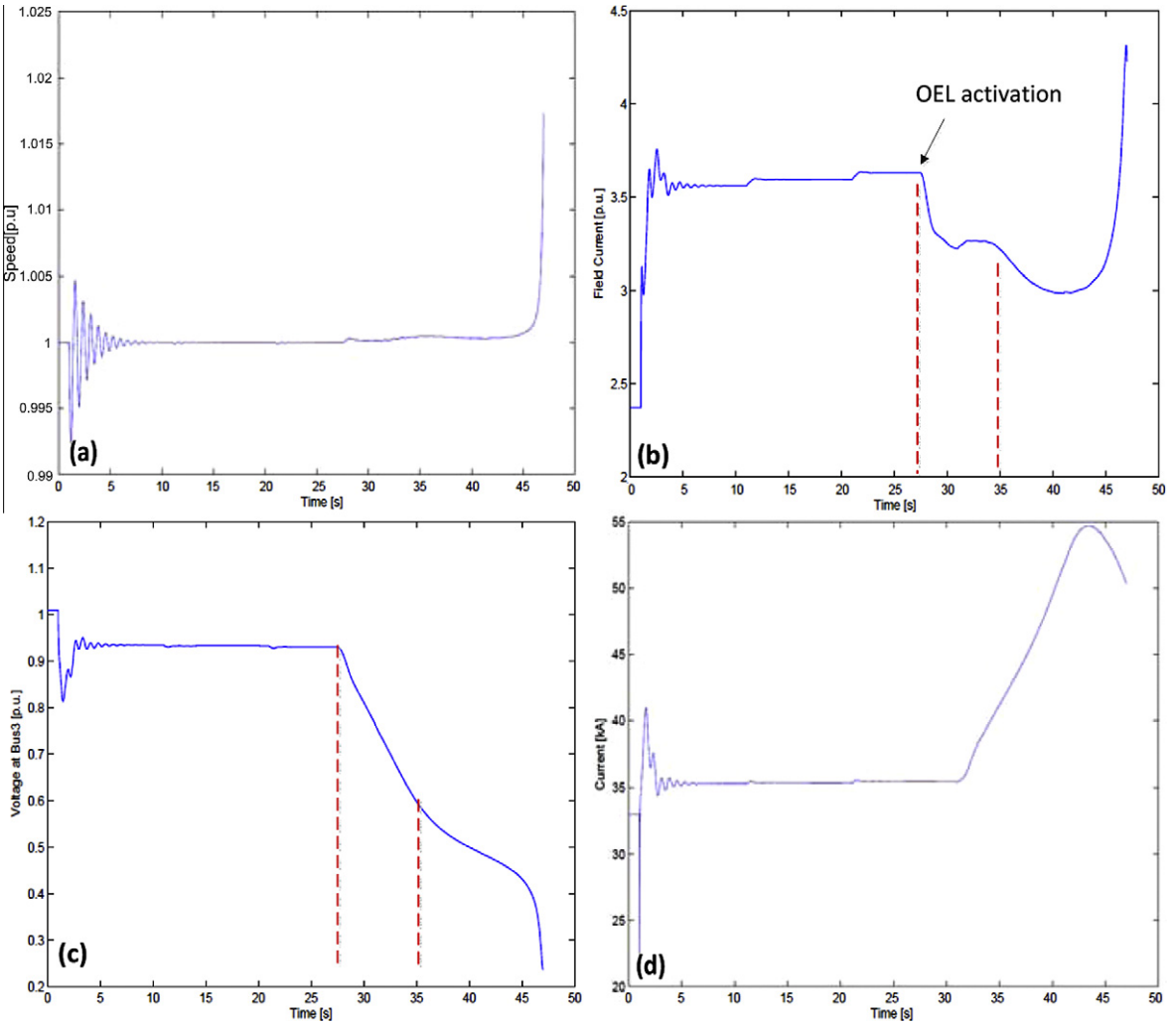

Fig. 21. Gen-speed (a), field current (b), voltage at Bus 3 (c) and motor-current (d).

paper briefly describes some common practices that must be considered when setting protective relays for power system. A short description of steps how to equip the "all-in-one" test system with commercial relays (available in software's library) in PowerFactory is described. The coordination of protective relays approach and optimization methodology between protection and control systems will be presented in detail for future work.

4.1. Considerations for the design of protective relays in the "all-in-one" system

- *The type of protective relay* should be selected so that it matches with the functional requirements and physical constrains of the power system. For instance, a distance (impedance) relay is suitable for transmission systems where multiple transmission corridor exist. In this paper, the "all-in-one" test system only has two transmission corridors, an the generation and load are matched radially. In this case, distance relays are not suitable because overcurrent protection is the major demand.
- *Size of the Current Transformer (CT)* should be selected to handle short-circuit currents without going into saturation. A common mistake to select a CT Ratio according to the MVA rating of the protected component, this is not the correct approach (for example, this approach does not take into account possible infeeds). A rule of thumb is to select CT ratios of 10 times smaller than the fault current, for example, 1000 A Fault current = 100/1 CT Ratio. For the secondary current, a rating of 1 A or 5 A can be selected depending on the distance between the transformer and the instrument it is feeding.

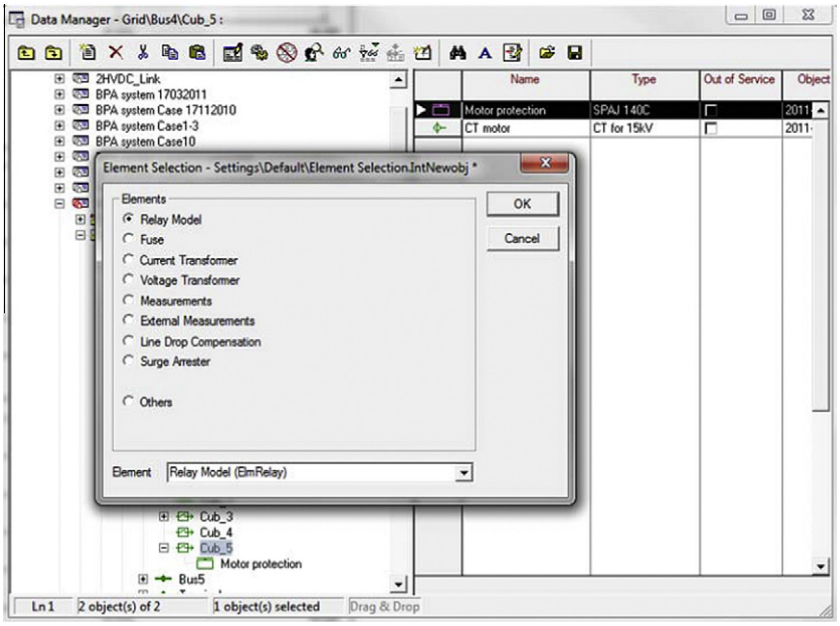

Fig. 22. Example of element selection window.

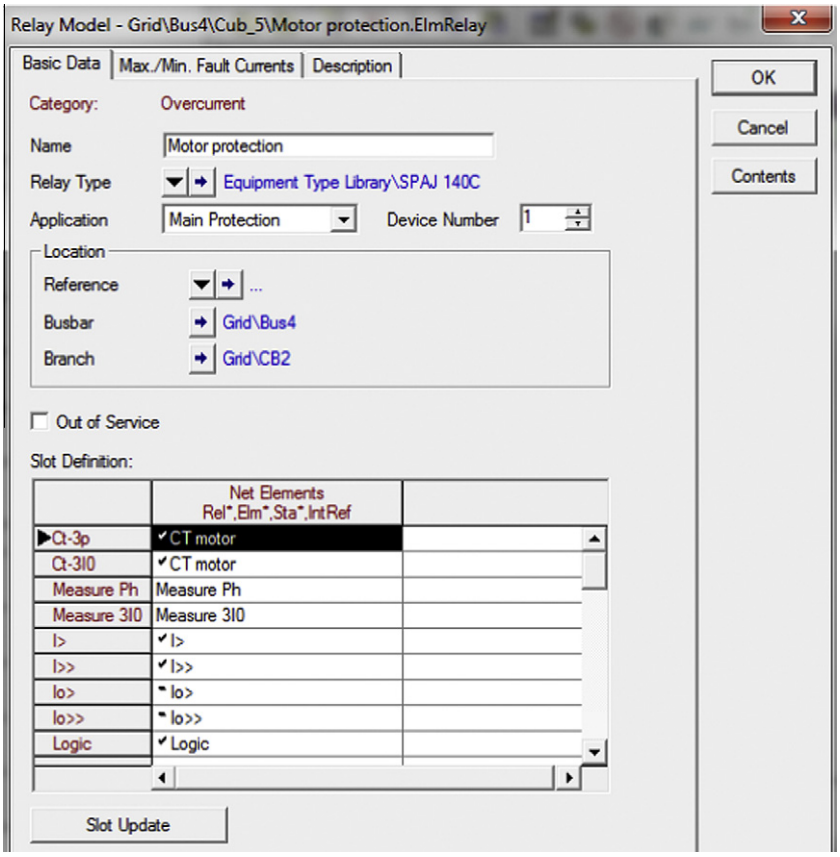

Fig. 23. Example of relay element setting window.

- *The motor's startup condition setting* must be pre-calculated for motor protection. In general terms, motor protection typically consists of 2–3 stages. The first stage is an instantaneous stage to clear faults on the connection cables or the motor windings. As the instantaneous tripping time is commonly smaller than the startup time of the motor, the pickup current has to be higher than the startup current (to prevent the relay from tripping on startup). The second stage is the running condition stage, which may be used to follow the motor characteristic more closely (as it is a stepped characteristic [19]). The third stage is an inverse characteristic to trip the motor during overloading periods, hence the time setting must to be chosen such that this stage does not trip while the motor is starting.

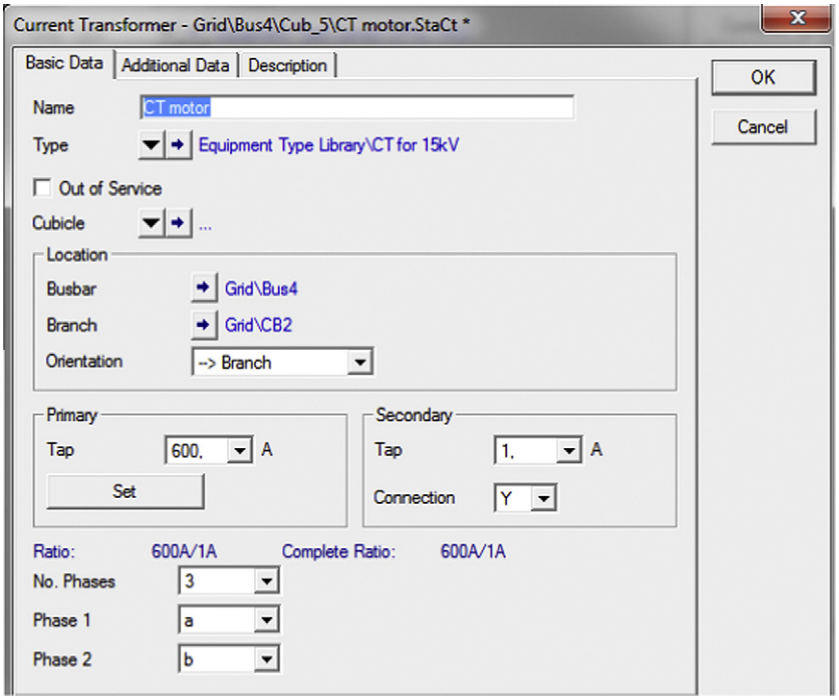

Fig. 24. Example of current transformer setting window.

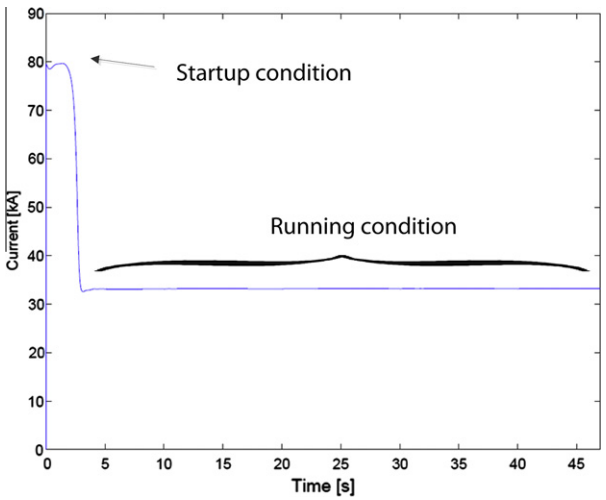

Fig. 25. Startup and running conditions of motor.

- *Selectivity*, defined in [20], is an overall design wherein only those protective devices closest to a fault will operate to remove the faulted component. This means the relay that is nearest to a fault location must send a trip signal to breakers to isolate a faulted component (isolating an as small as possible area around the fault position). For example, if there is a fault on the motor winding (see Fig. 1), only the motor should be disconnected from the system.

4.2. Steps to equip the "all-in-one" system with commercial relays

This section will provide a short description of each step to model protection devices in PowerFactory according to the common practices mentioned in Section 4.1. To this aim, we consider a short-term dynamic instability scenario that contains a motor load (which is documented in [18]). This scenario is similar to the long-term voltage instability phenomena mentioned earlier (see Section 3), however, part of the load at Bus 5 is shared with the motor load at Bus 4 while power generation is kept constant; whereas in Section 3 the motor load is disconnected. In this case, a long-term voltage instability triggers an instability of the short-term dynamics resulting in both loss of the generator's synchronism and motor stalling at $t = 47$ s (see Fig. 21a). The generator's OEL is activated at $t = 27$ s (see Fig. 21b). This results in an uncontrolled field voltage which is not able to restore the voltage at Bus 3 (see Fig. 21c). Finally, short-term voltage instability arises at $t = 35$ s, this is the ultimate cause of the system's collapse.

Fig. 21d depicts how the current magnitude of motor increases when the voltage at Bus 4 cannot be restored. The motor is overloaded by this current increase, hence one of the relays that can be chosen to protect this motor is an overcurrent relay. The steps to model an overcurrent motor protection relay in PowerFactory can be implemented as follows.

Step 1 – Insert a relay model and CT: A commercial relay from software library is first select. This model is then inserted to the bus's 'cubicle' to which the motor is connected by adding a new element in the "Data Manager" window where the simulation project has been created (see Fig. 22). Then "Element Selection" window will appear and elements such as relay model and CT can be added to the system. In this example, the ABB's SPAJ 140C is chosen.
Step 2 – Relay and CT settings: The settings can be prescribed by double-clicking the relay model that was added in Step 1, then the relay element window (shown as .ElmRelay) will appear (see Fig. 23). In this window, details such as relay type, location that relay is connected to (busbar and branch), and the settings of the relay's fault clearing stages can be modified. The relay's stages and CT setting can be set by double-clicking items in 'Net Elements' under 'Slot Definition' part. For instance, the CT for motor is selected and the setting window appears (see Fig. 24). In this window, the CT's setting

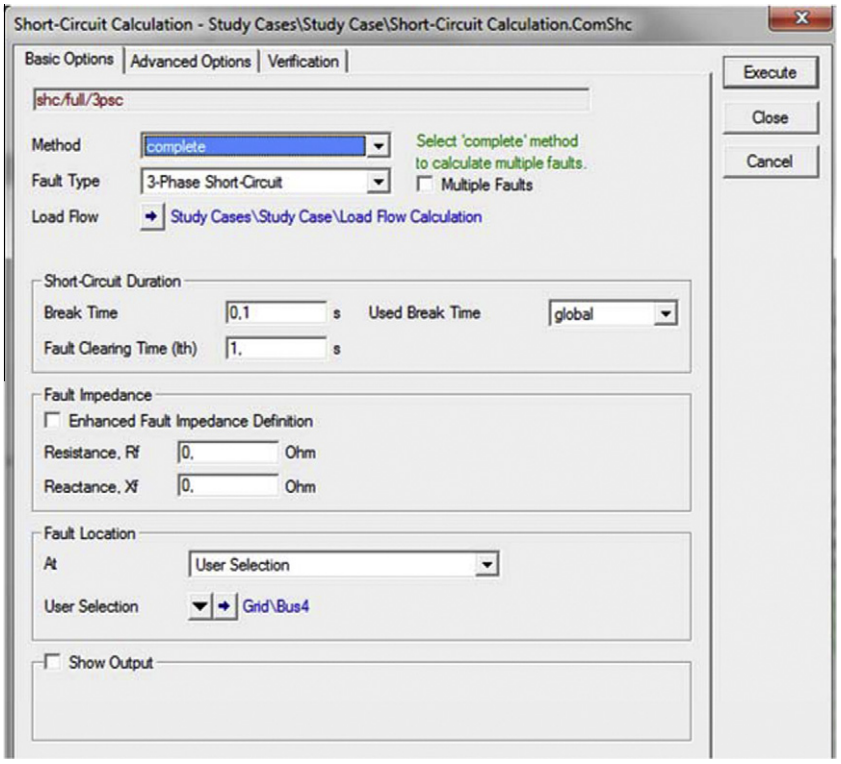

Fig. 26. Short-circuit calculation window.

such as primary and secondary tap ratio, and number of phase can be adjusted. The relay's fault clearing stages can be prescribed following a similar procedure as the one just described.

Step 3 – Verify the motor's startup and running conditions: A rule of thumb to select a motor's startup current is seven times the nominal motor current [21]. In the PowerFactory software, the startup current can be found by right-clicking the motor model, then the option "Calculation Motor Startup" will appear for determining motor's conditions. Fig. 25 shows the motor startup and running condition currents which are obtained in order to prescribe the appropriate settings of the associated protective relay.

The name of each stage indicate which kind of faults will be used. The symbol '$I>$' is used to clear remote faults (the relay acts as backup protection) or overloads. They generally have smaller current values but higher time settings to ensure selectivity with downstream relays. The symbol '$I\gg$' is used as an (nearly) instantaneous fault clearing stage in most cases. This means that the current values are very high (to ensure the fault is actually within the desired protection area) and within a short time range to clear these high currents. Therefore, it becomes necessary to set the '$I\gg$' stage to a value above the starting current (80 kA) and the '$I>$' to a value above the running condition (33 kA) but with a time setting above the motor startup time (which is approximately 5 s as shown in Fig. 25).

Step 4 – Verify the pickup current for the instantaneous fault clearing stage: This step is to confirm the pickup current setting of the '$I\gg$' stage. The value of the '$I\gg$' stage for the motor in the example discussed above can be set arbitrarily above 80 kA. Therefore, this most be modified so that the value used within the simulations is not set too high such that it will prevent a protection device to operate when there is a fault applied to the motor. In PowerFactory software, the

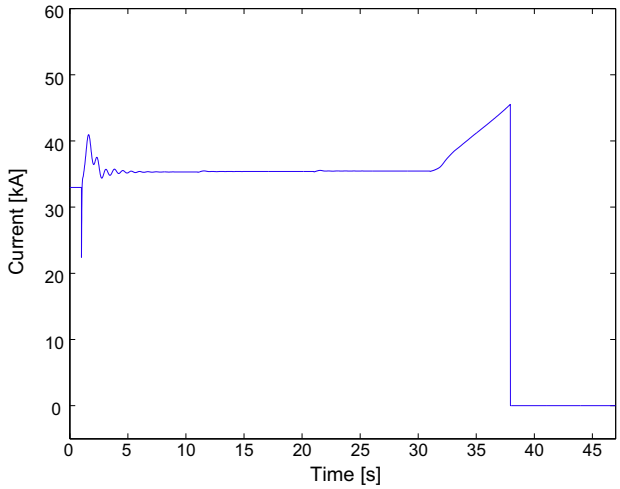

(a) Motor-Current

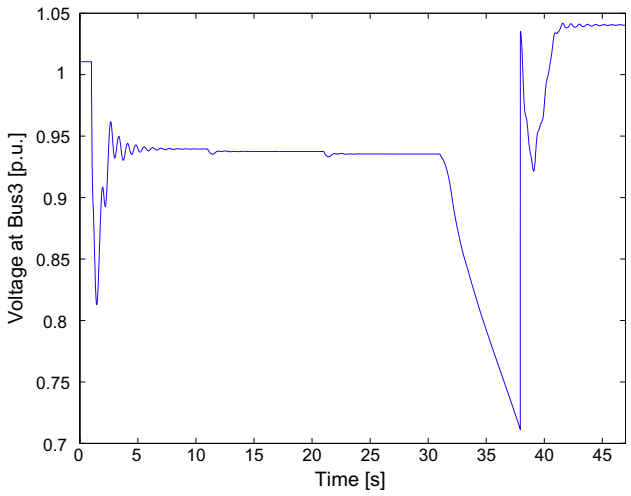

(b)VoltageatBus3

Fig. 27. Motor-current and voltage at Bus 3 traces showing the successful operation of a protective relay.

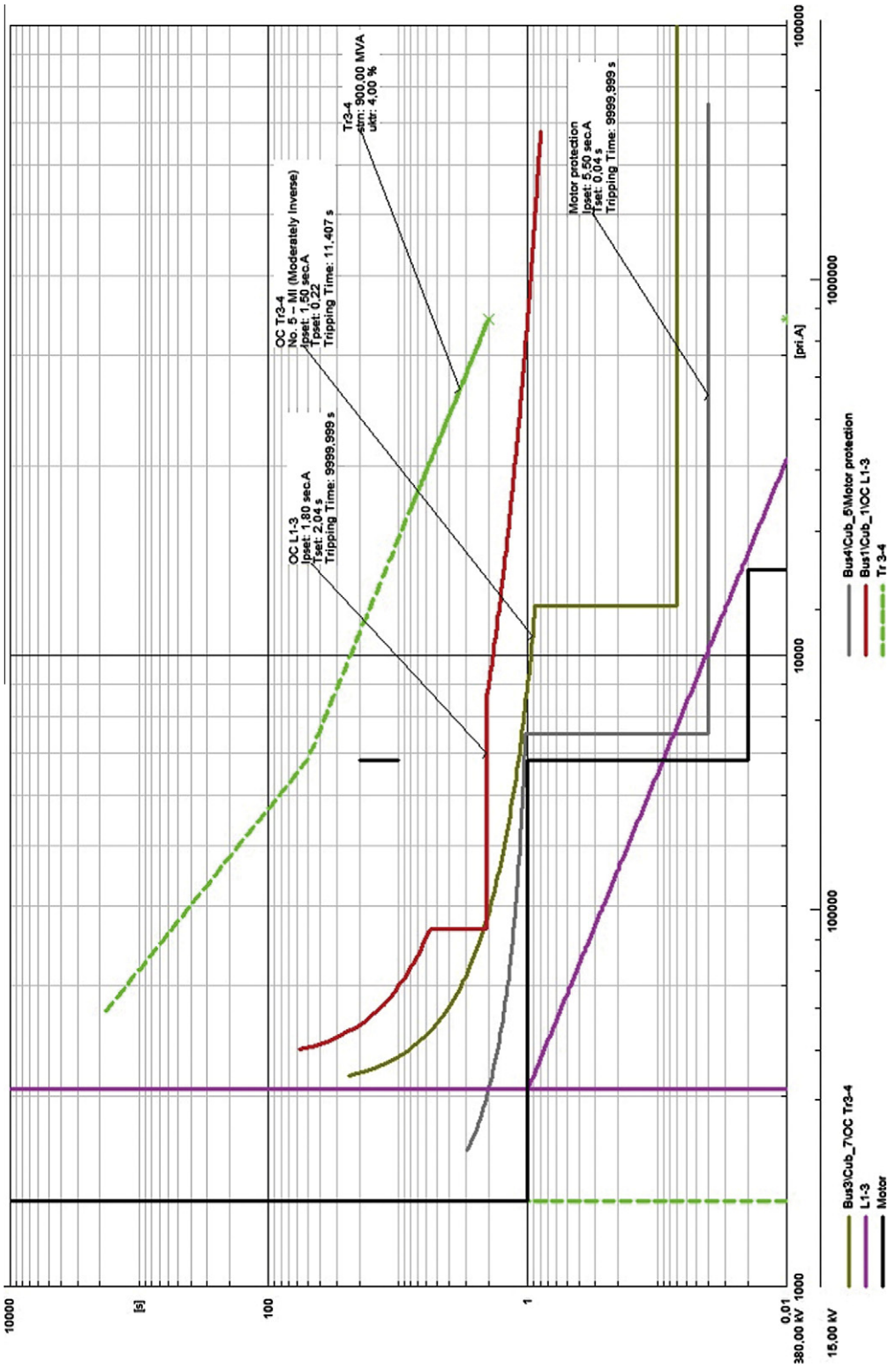

Fig. 28. Relay coordination time–overcurrent plot.

short-circuit calculation can be performed by right-clicking Bus 4 to which the motor is connected to, and by choosing the option "Calculation Short-Circuit" (see Fig. 26). All type of faults are available to determine short-circuit currents, and therefore, hence the minimum fault current can be calculated correctly so that the settings for the fault clearing stage can be prescribed correctly.

4.3. Simulation of the "all-in-one" test system considering protective relay operation

In this section it is shown how the careful implementation of protective devices within the "all-in-one" test system, described in the previous section, can successfully mitigate instabilities. To this aim, Fig. 27 shows that the motor protection relay successfully operates to disconnect the motor after a certain overloading period, hence the voltage at Bus 3 is able to be restored. In others words, the collapse of the "all-in-one" system is prevented.

A coordination of relays can be implemented in different ways according to, for example available types of relays or desired protection schemes which are dependent to different power systems. In this article, the relay coordination (see Fig. 28) for the test system can be conducted as follows.

1. An overcurrent (OC) relay is added to Bus 1 to protect line *L*1–3. The setting of instantaneous element must correspond to the maximum fault current and it should be higher than rating current of its protected line. Moreover, the setting should cover 80% along the total line length to ensure that the protection does not reach beyond into the response area of the next relay. The overloading characteristic can be set by calculating phase-to-phase fault using minimum short-circuit current. As shown in Fig. 28, the time–current characteristic of the relay represent in red line (*OC L*1–3). This tripping characteristic should lies on the right-hand side of the *L*1–3 (pink) line which represent the full-load current and overloading allowance of the line *L*1–3. For this particular example, the instantanous characteristic is set to trip at $t = 2$ s if the fault current reaches 1.8 times of the pick-up current while the overloading characteristic is set to 1.1 times of the pick-up current. The criterion of tripping characteristic for line *L*1–3*b* is expressed similarly but omitted for explanation purpose.
2. Another OC relay is added to protect transformer *TR*3–4 (Bus 3). In this case the setting of an overcurrent element has to be sensitive enough to see and clear a fault at high-voltage side of the transformer *TR*3–4. The tripping characteristic for transformer (see *OC TR*3–4 dark-green line) is similar to the line protection which explained earlier. However, the transformer damage curve (light-green-dash line) has to be checked in order to confirm that the tripping characteristic is sensitive enough to cover the transformer damage due to an maximum overloading capacity. The curve is set according the transformer rating and short-circuit voltage (in this example they are 900 MVA and 4%, respectively).
3. The last OC relay is added to protect the motor. If the setting of OC relay is set properly, the tripping characteristic should lie on the right-hand side of motor startup and running conditions (which explained earlier) that represented by black line in Fig. 28.

The coordination of all three relays should be set in such a way that the tripping characteristic of the component that is located the nearest (Line *L*1–3 in this case) to the generator should lie the right-most in the time–overcurrent plot. This means that if a fault occurs at the motor, the motor overcurrent relay should disconnect the motor from the system before other OC relays operate. Moreover, the tripping characteristic of each component should not overlap each other due to the selectivity considerations discussed in Section 4.1.

To illustrate relay-coordination for overcurrent protection, consider a three-phase short-circuit current applied on Transformer *TR*3–4 at $t = 10$ s, as shown in Fig. 28. According to the relay coordination settings shown, the OC relay disconnects the transformer at $t = 11.407$ s while the tripping time of other OC relays is equal to 9999.999 s. This coordination settings will result in the sole operation of *OCTR*3–4, and not other OC protection relays. Additional details for the design and simulation of other protection devices and functions in the "all-in-one" system will be presented in a future publication.

5. Conclusion

This paper presented a detailed modelling and implementation of a test system capable of generating different stability scenarios, including protective relays, within the commercial and proprietary power system simulation software DIgSILENT PowerFactory. Each of the device models were described and theoretical expressions were mapped to the different modelling and implementation approaches available within the software.

Simulation results show that the detailed modelling of each device is necessary to accurately represent the dynamic behaviour of the power system when is subject to different stability conditions. Moreover, a motor protection relay coordination was implemented and, it is shown that its operation is necessary to prevent a system collapse.

The coordination of protection devices and the accurate dynamic responses from the devices' detailed models will play a vital role for implementing advanced control algorithms. These algorithms will be capable of coordinating the operation of protective devices with power system controllers to improve power system stability.

Acknowledgment

The authors gratefully acknowledge the aid of Prof. Thierry Van Cutsem of the University of Liège for making available a MATLAB/Simulink test system from Ref. [6], which was used as a starting point for the work reported in this paper. His comments and suggestions for implementation within a commercial and proprietary power system simulation software are also gratefully acknowledged.

Appendix A. DSL code for LTC model implementation

```
1- t = time()
2- ! Initial value
3- Inc.(v0) = u
4- Inc.(nntap0) = nntapin
5- Inc.(tchangedown) = 0
6- Inc.(tchangeup) = 0
7- ! Definition of tap steps
8- tapdown = nntap0 − 1
9- tapup = nntap0 + 1
10- tapstop = 0
11- changeup = picdro({(u ∗ nntap0/nntapin) > (v0 + d)}, 0.0, 0.0)
12- changedown = picdro({(u ∗ nntap0/nntapin) < (v0 − d)}, 0.0, 0.0)
13- ! First step Delay
14- uplst = select(changeup = 1, 1.0, 0.0)
15- downlst = select(changedown = 1, 1.0, 0.0)
16- cond = select(picdro(uplst.or.downlst, 15, 0.0), 1, 0)
17- act = select(cond = 1, 1, 0)
18- later = act + 1
19- clear = select(picdro(later = 2, 0, 1000), 1, 0)
20- clearlst = select(clear = 1, 1, 0)
22- event(1, clearlst, 'create = EvtParam Target = this name = Deactivate_lst_change value = 0
  variable = act')
23- ! command to change Tap position = triggering
24- tchangedown = picdro({later > 1.and.nntap0 >= Tmin.and.changedown.and..not.delay(tchangedown,
  tdelay/15)}, tdelay, 0.0)
25- tchangeup = picdro({later > 1.and.nntap0 <= Tmax.and.changeup.and..not.delay(tchangeup, tdelay/
  15)}, tdelay, 0.0)
26- ! force event signal zero crossing
27- evtdown = tchangedown −0.5
28- evtup = tchangeup −0.5
29- nntapin = nntap0
30- lim(select(evtdown, nntap0 − 1, select(evtup, nntap0 + 1, nntap0)), Tmin, Tmax)
31- ! set event
32- event(0, evtdown, 'name = this dtime = 0. value = tapdown variable = nntap0')
33- event(0, evtup, 'name = this dtime = 0. value = tapup variable = nntap0')
34- ! Check the difference
35- tstop = picdro({abs((u ∗ nntap0/nntapin) − v0) < 0.01}, 3.0, 0.0)
36- evtstop = picdro(evtstop > 0.and.t > 20, 0.0, 0.0)
37- event(0, evtstop, 'name = stoptap dtime = 0. value = nntap0 variable = nntapin')
38- check = (u ∗ nntap0/nntapin)
39- vardef(Tmin) = 'p.u.'; 'Min Tap Position'
40- vardef(Tmax) = 'p.u.'; 'Max Tap Position'
41- vardef(d) = '%'; 'LTC half volt deadband'
42- vardef(tdelay) = 's'; 'Delay between 2 subsequent stap change'
43- vardef(umin) = 'pu'; 'Min Voltage'
44- vardef(umax) = 'pu'; 'Max Voltage'
```

Appendix B. Initial condition setting for the long-term voltage instability phenomena

bus 1:	V = 1.0800 pu	0.00 deg	410.40 kV
>1–3	P = 600.0	Q = 216.7	>3
>1–3b	P = 600.0	Q = 216.7	>3
gener 1	P = 1200.0	Q = 433.5	Vimp = 1.0800
bus 2:	V = 1.0100 pu	−14.79 deg	20.20 kV
>2–3	P = 300.0	Q = 212.6	>3
gener 2	P = 300.0	Q = 212.6	Vimp = 1.0100
bus 3:	V = 1.0166 pu	−17.58 deg	386.30 kV
>1–3	P = −600.0	Q = −23.9	>1
>1–3b	P = −600.0	Q = −23.9	>1
>2–3	P = −300.0	Q = −191.4	>2
>3–4	P = 0.0	Q = 0.0	>4
>3–5	P = 1500.0	Q = 239.3	>5
bus 4:	V = 0.9966 pu	−17.58 deg	14.95 kV
>3–4	P = 0.0	Q = 0.0	>3
gener 4	P = 0.0	Q = 0.0	Vimp = 0.0000
bus 5:	V = 1.0089 pu	−20.93 deg	383.37 kV
>3–5	P = −1500.0	Q = −150.0	>3
load	P = 1500.0	Q = 150.0	

References

[1] S. Larsson, E. Ek, The blackout in Southern Sweden and Eastern Denmark, September 23, 2003, Power Engineering Society General Meeting, 2004, vol. 2, IEEE, 2004, pp. 1668–1672.
[2] US–Canada Power System Outage Task Force, 2004, Final Report on the August 14, 2003 Blackout in the United States and Canada: Causes and Recommendations. <http://www.nerc.com>.
[3] S. Corsi, C. Sabelli, General blackout in Italy Sunday September 28, 2003, h. 03:28:00, Power Engineering Society General Meeting, 2004, vol. 2, IEEE, 2004, pp. 1691–1702.
[4] Preliminary Report into the Recent Electricity Transmission Faults affecting South London and East Birmingham, Tech. Rep., Office of Gas and Electricity Market, OFGEN, 30 September, 2003.
[5] R. Leelaruji, L. Vanfretti, M. Ghandhari, L. Söder, Coordination of protection and VSC-HVDC systems for mitigating cascading failures, in: 2010 International Conference on Power System Technology (POWERCON), IEEE, New York, 2010, pp. 1–8, doi:10.1109/POWERCON.2010.5666604.
[6] C.D. Vournas, E.G. Potamianakis, C. Moors, T. Van Cutsem, An educational simulation tool for power system control and stability, IEEE Transactions on Power Systems 19 (1) (2004) 48–55.
[7] F. Milano, L. Vanfretti, State of the art and future of OSS for power systems, in: IEEE Power Energy Society General Meeting, IEEE, New York, 2009, pp. 1–7, doi:10.1109/PES.2009.5275920.
[8] A. Murdoch, G. Boukarim, M. D'Antonio, J. Zeleznik, Use of the latest 421.5 standards for modeling today's excitation systems, in: IEEE Power Engineering Society General Meeting, vol.1, IEEE, New York, 2005, pp. 989–994. doi:10.1109/PES.2005.1489673.
[9] Digital Excitation Task Force of the Equipment Working Group, Computer Models for Representation of Digital-Based Excitation Systems, IEEE Transactions on Energy Conversion 11 (1996) 607–615.
[10] IEEE Standard 421.5-2005, IEEE Recommended Practice for Excitation System Models for Power System Stability Studies.
[11] IEEE Committee Report, Dynamic Models for Steam and Hydro Turbines in Power System Studies, IEEE Transactions on Power Apparatus and Systems PAS-92 (1973) 1904–1915.
[12] IEEE Task Force on Excitation Limiters, Recommended Models for Overexcitation Limiting Devices, IEEE Transactions on Energy Conversion 10 (1995) 706–713.
[13] T. Van Cutsem, C. Vournas, Voltage Stability of Electric Power Systems, Kluwer Academic Publisher, 1998.
[14] CIGRE Task Force 38-02-10. Modelling of Voltage Collapse Including Dynamic Phenomena, 1993.
[15] P.W. Sauer, M.A. Pai, A comparison of discrete vs. continuous dynamic models of tap-changing-under-load transformers, in: Proceedings of NSF/ECC Workshop on Bulk power System Voltage Phenomena - III: Voltage Stability, Security and Control, Davos, Switzerland, 1994.
[16] DIgSILENT PowerFactory Version 14. URL. <http://www.digsilent.de/>.
[17] P. Kundur, J. Paserba, V. Ajjarapu, G. Andersson, A. Bose, C. Canizares, N. Hatziargyriou, D. Hill, A. Stankovic, C. Taylor, T. Van Cutsem, V. Vittal, Definition and classification of power system stability IEEE/CIGRE joint task force on stability terms and definitions, IEEE Transactions on Power Systems 19 (3) (2004) 1387–1401.
[18] R. Leelaruji, L. Vanfretti, All-in-One Test System Modelling and Simulation for Multiple Instability Scenarios, Internal Report, KTH, Royal Institute of Technology, April, 2011.
[19] ABB, Motor Protection REM 545. <http://www05.abb.com/global/scot/scot229.nsf/veritydisplay/5af37b57b42ddcb7c12577c9002b9411/$file/rem54_tob_751173_enh.pdf>.
[20] P. Andersson, Power System Protection, Wiley-IEEE Press, 1998.
[21] T. Schoepf, R. Rowlands, G. Drew, Contact welding at break of motor inrush current, IEEE Transactions on Components and Packaging Technologies 29 (2006) 278–285.